

## Contact Pressure in Dynamic Compression of Clay Specimens

and Its Application to Sheet Metal Forming\*

by Katsumi YAMAGUCHI\*\*, Yasushi KUROSAKI\*\*\*,

Minoru MAEDA' and Yasushi KODAMA''

A new method for sheet metal forming which utilizes the strain-rate dependence of flow stress in the viscoplastic material and the friction-hill phenomenon is proposed. In order to assess its applicability, a dynamic compression test of clay specimens is carried out using a drop hammer apparatus, and the contact pressure on the specimen-platen interface is examined. It is concluded that the proposed method is applicable to sheet forming for relatively small articles. Based on experimental and theoretical considerations, a simple method for estimating the maximum pressure generated under any condition is presented. Some applications of the process to sheet metal forming are shown.

Key Words : Forming, Clay Specimen, Dynamic Compression Stress, Viscoplastic Body, Contact Pressure, Batch Production, Sheet Metal Forming.

## 1. Introduction

Recently, because of the demand for conserving natural resources and energy and the increasing variety of industrial items, the establishment of a production system suitable for multiple and small lots has become one of the important problems to be solved at stamping shops. Thus, flexible sheet-forming processes which employ rubber or fluid as a pressure-transmitting medium have been recognized anew mainly for economical reason<sup>(1)(2)</sup>. Generally speaking, rubber is convenient in usage but inferior to fluid in fluidity, pressure-transmitting ability and recycling after age or damage due to severe deformation. On the other hand, fluid requires special devices for sealing and pressurizing.

The final aim of the present research is to develop a sheet forming process which employs a medium with none of the problems aforementioned which is applicable to small batch production. By way of trial, a method which utilizes the high strain-rate dependence of flow stress in viscoplastic materials is taken up here. Its schematic drawing is shown in Fig. 1. Sheet forming is achieved with a high pressure generated by impulsively compressing a viscoplastic material; thus the punch and the blank-holder can be dispens-

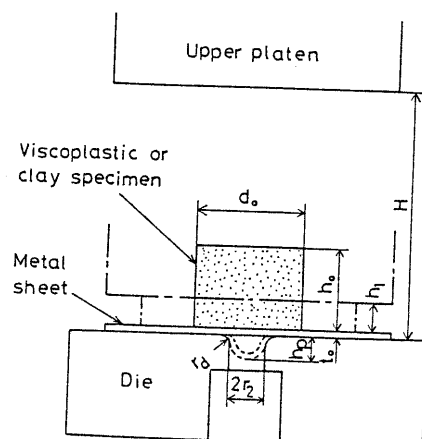


Fig. 1 Schematic drawing of the stretch-forming process employing a viscoplastic medium.

ed with. As the first step for the purpose the contact pressure in dynamic compression of clay specimens will be examined and the applicability of the proposed process will be discussed. Its application will also be presented.

## 2. Experimental Procedure

## 2.1 Apparatus

The drop hammer apparatus used is of free-fall type. The total mass of the hammer including the upper platen  $M$  was changed from 39.6 kg to 85.2 kg in steps of about 9 kg, and its fall height was continuously changed from zero to 172 cm.

In order to obtain fundamental information about the pressure, a dynamic simple compression test of clay specimens was made, neglecting the plastic deformation of sheets, and the contact pressure on the specimen-platen interface was examined. For this purpose, a pressure-sensitive pin

\* Received 25th October, 1982.

\*\* Professor, Faculty of Engineering, Nagoya University, Furo-cho, Chikusa-ku, Nagoya.

\*\*\* Associate Professor, Faculty of Engineering, Mie University, 1515 Kamihama-cho, Tsu, Mie-ken.

' Tsurumi Factory, Toshiba Corporation, 2-4 Suehiro-cho, Tsurumi-ku, Yokohama.

'' Graduate Student, Faculty of Engineering, Mie University, 1515 Kamihama-cho, Tsu, Mie-ken.

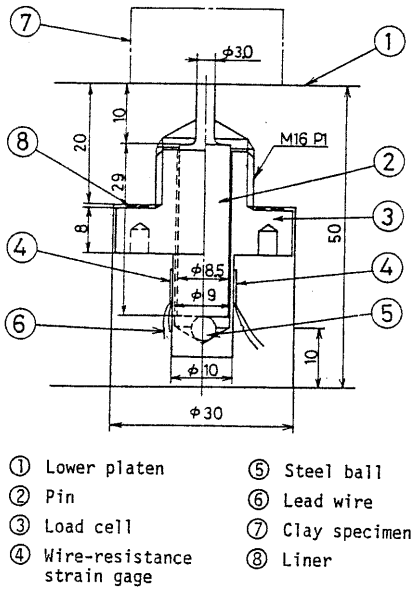


Fig. 2 Pressure-sensitive pin apparatus.

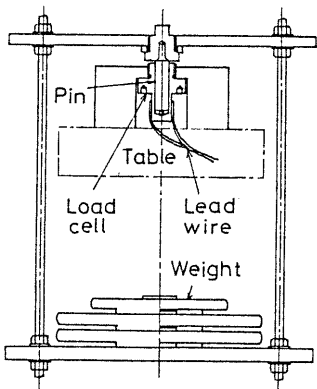
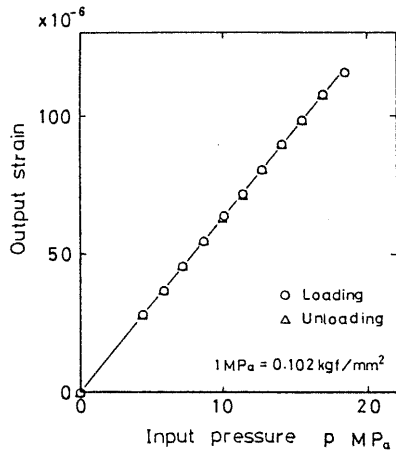


Fig. 3 Calibration method of pressure and the calibrated result.

apparatus having a maximum capacity of 60 MPa (612 kgf/cm<sup>2</sup>) was provided in the lower platen, as shown in Fig. 2 and pressure-time curves were recorded on an electromagnetic oscillograph. The measurement of the pressure at each radial position was accomplished by shifting the lower platen relative to the specimen and the hammer so that the pin might be located there eccentrically with them. An outline of the calibration method of pressure and the calibrated result are shown in Fig. 3, where a good linear relation is observed throughout the loading and unloading processes. The height of the protruding part of the pin above the platen surface was detected with a stylus instrument (TALYSURF 10) and adjusted to the range of  $\pm 3 \mu\text{m}$ . An example of the pressure-time curve recorded is shown in Fig. 4; hereafter the pressure peak will be noted and denoted as  $p$ .

Within the present experimental condition, the response frequency of the apparatus was at least 5 times as large as the pressure frequency and thus was regarded as enough for the present purpose. Though not stated here, the  $p$  value was compared with the pressure obtained from the stretch method using metal foils and a die with a very small aperture, and its

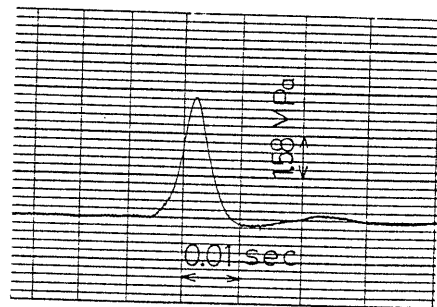


Fig. 4 An example of the pressure-time curve recorded.

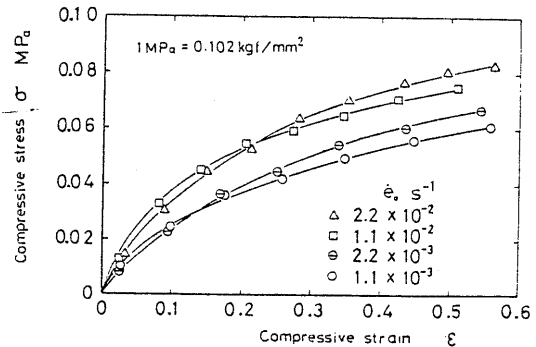


Fig. 5 Stress-strain curves in the quasi-static compression test of clay specimens.

Table 1 Tensile properties of Al050-H24 sheet.

Orientation to rolling direction	n-value	Tensile strength		Total elongation %
		F MPa {kgf/mm <sup>2</sup> }	MPa {kgf/mm <sup>2</sup> }	
0°	0.02	142 {14.5}	133 {13.6}	8.7
45°	0.02	143 {14.6}	134 {13.7}	
90°	0.01	145 {14.8}	136 {13.9}	2.5
Mean	0.02	144 {14.7}	134 {13.7}	6.9
				5.2

$t_o = 0.2 \text{ mm}, \sigma = F \epsilon^n.$

reliability was confirmed.

2.2 Clay Material and Specimens

The material employed as a pressure-transmitting medium is commercial clay (blue, density  $\rho = 1.91 \text{ g/cm}^3$ , bulk modulus  $K = 2940 \text{ MPa}$ ), which is composed of powder (lime and pyrophyllite), mineral oil and additives (wax, surface-active agent, pigment, etc.) with a weight ratio of 7 (powder) : 3 (mineral oil + additives). Its quasi-static compressive stress ( $\sigma$ ) - compressive strain ( $\epsilon$ ) curves are illustrated in Fig. 5. Lubricants used are graphite grease and PTFE sheet 0.05 mm in thickness. The value of  $\sigma$  is very low in the range of tested strains and strain-rates; even the maximum is nearly equal to 0.08 MPa. Clay cylinders, referred to as specimens hereafter, were manufactured by means of a forming device and kept at room temperature for one night before testing. Their diameters  $d_o$  were 20, 40, 60 and 80 mm, and their relative heights  $h_o/d_o$  ranged from 0.065 to 2.15. Each surface of platens was lap-finished to a surface roughness of  $0.5 \mu\text{mR}_{\text{max}}$ . It was degreased with acetone before testing, but no lubricants were used. The test temperature was  $20 \pm 5 \text{ }^\circ\text{C}$ .

2.3 Metal Sheets

Commercially pure aluminum sheets with half-hard quality (A 1050-H24, 0.2 mm thick) were used for forming tests. Their tensile properties are shown in Table 1, where each mean value  $\bar{X}$  was calculated with the equation  $\bar{X} = (X_0 + 2 X_{45} + X_{90})/4$  and  $X_0, X_{45}$  and  $X_{90}$  were measured with the tensile specimens cut at 0°, 45° and 90° to the rolling direction, respectively. The surface roughness of the sheets were  $0.6 \mu\text{mR}_{\text{max}}$  in the rolling direction and  $0.5 \mu\text{mR}_{\text{max}}$  in the direction perpendicular thereto.

3. Factors Influencing Contact Pressure  $p$

The radial distributions of  $p$  are shown for various combinations of the hammer mass  $M$ , its fall height  $H$ , the initial diameter of the specimen  $d_o$  and its relative height  $h_o/d_o$  in Fig. 6. The effect of the specimen volume  $V_o$  on  $p$  can be examined by comparing the results for the case numbers denoted by 1 and 2 in the figure, while 2 and 3 give the effect of  $H$

; similarly, 4 and 5 indicate the effect of  $M$  under the constant potential energy of the hammer. In the present experiment  $p$  always showed a tendency to decrease with an increase of the radial position  $r$ , and its maximum was found near the specimen center ( $r = 0 \text{ mm}$ ), as seen in Fig. 6. Thus it is thought to utilize effectively  $p$  at this region, denoted as  $p_o$  hereafter, for sheet metal forming. Figure 7 shows the plots of  $p_o$  versus  $h_o/d_o$  for various combinations of  $H$  and  $V_o$ . It is found from Figs. 6 and 7 that  $p_o$  has been enhanced by increasing  $H$  and  $M$  and by decreasing  $V_o$  and  $h_o/d_o$ .

These results suggest that the proposed method facilitates generation of a considerable pressure magnitude by selecting the factors, i.e.,  $H, M, V_o$  and  $h_o/d_o$ . Though an upper limit of  $p_o$  has not been determined yet, 60 MPa ( $612 \text{ kgf/cm}^2$ ), the maximum value measurable with the present apparatus, has been attained without any difficulty. Accordingly, the method seems applicable to a certain sheet forming. However, considering that the high pressure region is limited to near the specimen center, it is recommended for stretch-forming, embossing and bending of small articles.

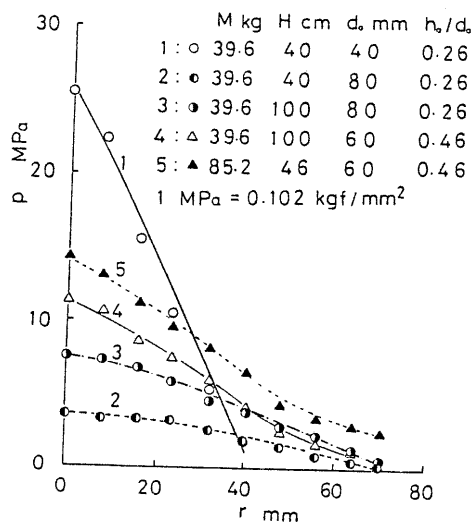


Fig. 6 Pressure distribution in the radial direction.

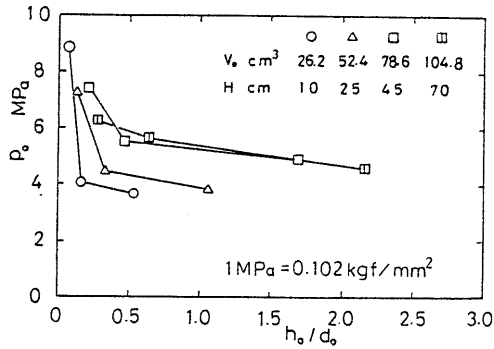


Fig. 7 Relation between the maximum pressure  $p_o$  and the relative height of the specimen  $h_o/d_o$ .

4. Estimation of Maximum Pressure  $p_o$

Based on the need for determining the forming condition, a method for estimating  $p_o$  is given in the following.

4.1 Introduction of Mean Compressive Stress

Concerning dynamic flow stresses of metals, plasticine and other model materials, many investigations have been made before (4)~(7). Aku and his co-workers proposed the following simplified procedure for evaluating the mean compressive stress  $Y_m$  and applied it to plasticine (5).

By the principle of conservation of momentum, we have

$$v = \{M/(M+m)\}v_o \tag{1}$$

where  $v_o = \{\sqrt{2g(H-h_o)}\}$  and  $v$  are the hammer velocities just before and after impacting, respectively;  $g$  is gravitational acceleration, and  $M$  and  $m$  are masses of the hammer and the specimen, respectively. Deformation time  $t_1$  and the strain rates based on the expressions of the nominal and natural strains, denoted by  $\dot{\epsilon}_m$  and  $\dot{\epsilon}_n$  respectively, are defined as

$$t_1 = (h_o - h_1)/(1/2v) \tag{2}$$

$$\dot{\epsilon}_m = e_1/t_1 = \{(h_o - h_1)/h_o\}/t_1 = v/(2h_o) \tag{3}$$

and

$$\begin{aligned} \dot{\epsilon}_n &= \epsilon_1/t_1 = 1_n(h_o/h_1)/t_1 \\ &= \dot{\epsilon}_m \epsilon_1 / (1 - e^{-\epsilon_1}) \end{aligned} \tag{4}$$

where  $e_1$  and  $\epsilon_1$  are the nominal and natural compressive strains due to positive definition, and  $e$  is the base of the natural logarithm. By the rule of impulse, the mean compressive force  $F_m$  is written as

$$F_m = (M+m)v/t_1 = Mv_o/t_1 \tag{5}$$

Noting  $m \ll M$  in the present experiment and putting  $v \approx v_o$ , we find from Eqs. (2) and (5)

$$F_m \approx (1/2)Mv_o^2/(h_o - h_1) \tag{5'}$$

The mean compressive stress  $Y_m$  is defined as

$$Y_m = F_m/A_m = (h_o + h_1)F_m/(2V_o) \tag{6}$$

where  $A_m$  is the mean area of the transverse cross section of the specimen and  $V_o$  is its volume. The stress  $Y_m$  corresponds to the mean value in regard to the radial position and deformation process, and can be easily calculated for any shape of the cross section from Eqs. (5)' and (6), if only the final specimen height  $h_1$  is known. According to Fig. 8 showing the relation between  $Y_m$  and  $p_o$ , the proportional relation

$$p_o = 2.92 Y_m \tag{7}$$

approximately holds. This suggests that if  $Y_m$  is known, an approximate value of  $p_o$  can be predicted from Eq. (7).

4.2 Estimation of  $Y_m$

For the estimation of  $Y_m$ , we have to know in advance either the final height of a specimen  $h_1$  or a compressive strain  $\epsilon_1$ .

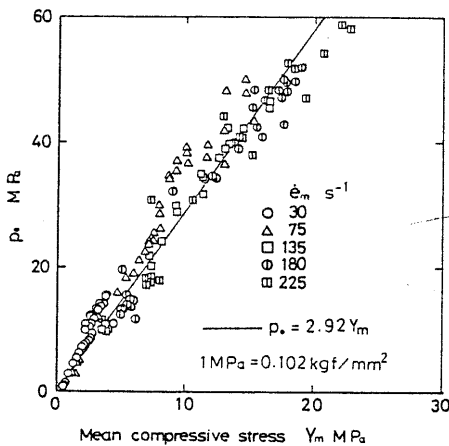


Fig. 8 Experimental relation between  $p_o$  and the mean compressive stress  $Y_m$ .

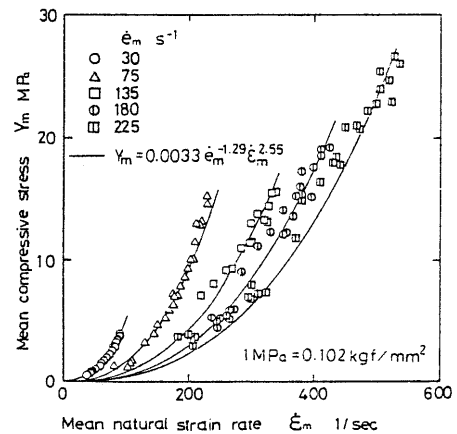


Fig. 9 Relation between  $Y_m$  and  $\epsilon_m$ .

Of course, it may be obtained directly from the experiment, but a theoretical procedure of a more general character will be presented in the following.

Quoting the constitutive equation employed sometimes in hot working of metals, Aku and his co-workers<sup>(5)</sup> reported that  $Y_m = c\dot{\epsilon}_m^\alpha$  holds for plasticine. However,  $Y_m$  in this experiment was found to be dependent not only on  $\dot{\epsilon}_m$  but also on  $\epsilon_1$ , and thus the following equation was regarded as more applicable.

$$Y_m = c\dot{\epsilon}_m^\alpha \epsilon_1^\beta \quad (8)$$

Figure 9 shows the plots of  $Y_m$  versus  $\dot{\epsilon}_m$  for various combinations of  $H$ ,  $d_o$  and  $h_o/d_o$  but under constant  $M$  ( $=39.6$  kg). Curves drawn in the figure are based on the equation  $Y_m = 0.0033\dot{\epsilon}_m^{-1.29}\epsilon_1^{2.55}$  (MPa), determined by the least square method, and they correspond fairly well to the experimental plots. A similar relation was confirmed for plasticine. Such discrepancy between the results by the authors and Aku et al. seems to be due to the lubricants employed. From Eqs. (4) and (8), it is seen that  $Y_m$  has a positive correlation with  $\dot{\epsilon}_m$  (or  $\epsilon_1$

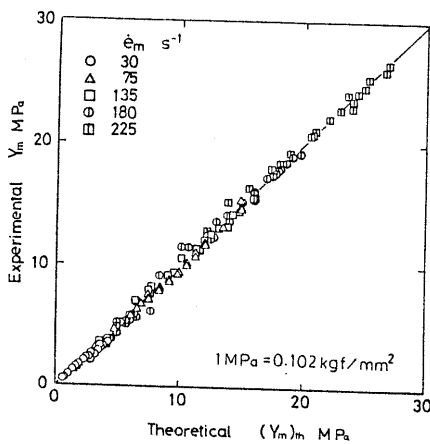
) and  $\epsilon_1$ . The former correlation is considered to be due to the viscosity of the clay, while the latter is attributed to the friction on the specimen-platen interface. With respect to the mechanical properties of the clay material, higher  $c$  and  $(\alpha + \beta)$  values are desirable for the proposed process, because they serve to enhance  $Y_m$  and therefore  $p_o$ . From Eqs. (6) and (8) we obtain

$$A\left(1 - \frac{h_o}{H}\right) + \frac{1 - e^{\epsilon_1}}{1 + e^{\epsilon_1}} \left(\frac{\epsilon_1}{1 - e^{-\epsilon_1}}\right)^\beta = 0 \quad (9)$$

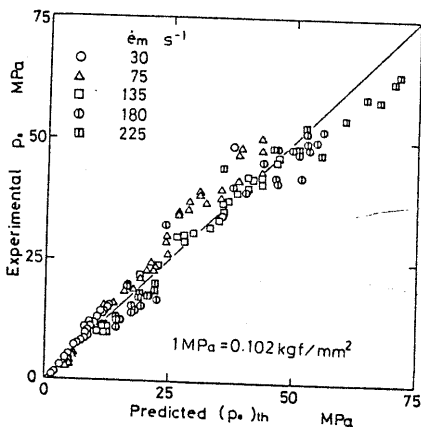
where  $A = MgH / (2V_o c \dot{\epsilon}_m^{\alpha+\beta})$ . When the constants  $c$ ,  $\alpha$  and  $\beta$  are determined by performing a dynamic compression test specifying  $\dot{\epsilon}_m$ ,  $\epsilon_1$  can be obtained for any impulse condition by solving numerically Eq. (9). In this research  $\epsilon_1$  was calculated by the Newton method and then  $Y_m$  was determined from Eqs. (5)' and (6), and subsequently  $p_o$  from Eq. (7). The theoretical values of  $Y_m$  and  $p_o$  are compared with the experimental ones in Figs. 10 (a) and (b), respectively, which show that  $Y_m$  can be predicted with enough accuracy and  $p_o$  within an error of  $\pm 10$  percent.

#### 4.3 Consideration of $p_o - Y_m$ Relation

In order to examine the material flow in the specimen, a ring specimen made of black clay was inserted into a blue specimen, as shown in Fig. 11 (a). The vertical cross section of the compressed specimen is presented in Fig. 11 (b); a very little radial flow is observed at the specimen ends, which indicates that a very high friction has occurred there. A similar phenomenon was pointed out in an early experiment for plasticine<sup>(5)</sup>. On the other hand, a large material flow is seen inside the specimen. A strict theoreti-

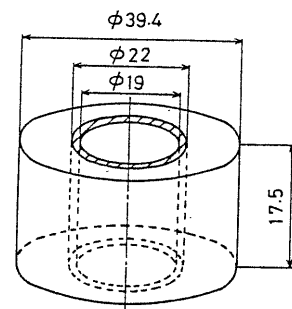


(a)  $Y_m$



(b)  $p_o$

Fig. 10 Comparison between theoretical and experimental  $Y_m$  and  $p_o$  values.



(a) Initial specimen



(b) After compression ( $H = 5$  cm,  $M = 39.6$  kg)

Fig. 11 Observation of the material flow in the specimen.

cal consideration taking account of these deformation states is not made here, but a simple theory is quoted.

Referring to the elementary solution<sup>(3)</sup> assuming stick friction on the specimen-platen interface, the relation between the pressure at the specimen center  $p_o$  and the mean compressive stress  $\bar{Y}$  in axi-symmetrical upsetting is written as

$$p_o = D_1 \bar{Y}, \quad D_1 = (1 + D_2) / (1 + D_2/3) \quad (10)$$

where  $\bar{Y} = \left( \int_0^r 2\pi\xi p d\xi / (\pi r^2) \right)$  is averaged

in regard to the radial position,  $D_2 = (2/\sqrt{3})(r/h) = (2/\sqrt{3})(r_o/h_o)e^{\epsilon}$ ,  $r$  and  $h$  are the current radius of the specimen and its current height, respectively, and  $\epsilon$  is a compressive strain. Equation (10) is true for the quasi-static condition. Though a similar equation taking account of inertia can be derived for the dynamic problem<sup>(8)</sup>, its effect on  $D_1$  was estimated as negligibly small, say about 1 percent, in the present condition.

We next apply Eq. (10) to our compression problem. The relation between  $\bar{Y}$  and  $\epsilon$  has not been examined experimentally, but is derived theoretically as Eq. (17) in the appendix on the basis of the constitutive equation  $\bar{Y} = c' \dot{\epsilon}^p \epsilon^q$ . Substituting the expression for  $\bar{Y}$  from Eq. (17) into Eq. (10) gives  $p_o$  for any value of  $\epsilon$ . On the other hand,  $Y_m$  can be obtained from Eqs. (5)', (6) and (16). According to the computed result,  $p_o$  attained a maximum at  $\epsilon = (1/2) \epsilon_1$ , irrespective of  $d_o$ ,  $h_o/d_o$  and  $H$ . The theoretical relation between  $p_o$  and  $Y_m$  is shown in Fig. 12, where they are plotted near the line  $p_o = 3Y_m$  throughout the examined cases. In this way, Eq. (7) has proved to be mechanically possible, and after all it can be pointed out that such a relation is limited to the cases of very large deformation ( $\epsilon_1 = 0.6 \sim 3.0$ ) and high friction. A further calculation indicated that  $Y_m$  is not identical with the strict mean stress  $Y_{mean} = \int_0^{\epsilon_1} \bar{Y} d\epsilon / \epsilon_1$

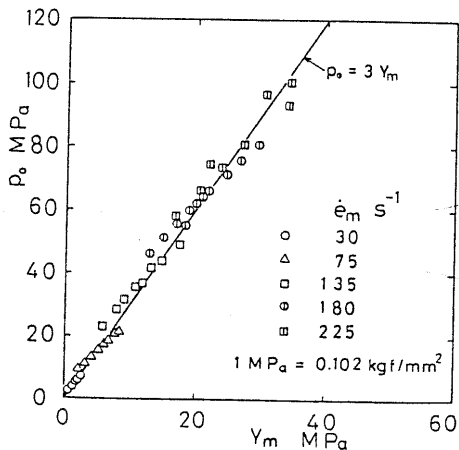


Fig. 12 Calculated relation between  $Y_m$  and  $p_o$ .

but is 20 ~ 30 percent larger than the latter. However, since the authors' method for estimating  $p_o$  does not require coincidence between them, no problem is involved. The stress  $Y_m$  is regarded as a simple and useful mechanical measure.

#### 4.4 Estimation of Hammer Fall Height in Stretch-Forming

Using the aforementioned procedure for predicting  $p_o$ , let us estimate the fall height of the hammer  $H$  necessary to achieve stretch-forming for metal sheets. The pressure  $p$  corresponding to a specified forming height  $h_p$  was calculated from Takahashi's equation<sup>(9)</sup> for the hydrostatic bulging process, and then  $H$  was determined by reverse calculation on the basis of the theory mentioned in sections 4.1 and 4.2, putting  $p_o = p$ . The comparison between the estimated and experimental results for A 1050-H24 sheets is made in Fig. 13, where the die aperture and profile radii,  $r_2$  and  $r_d$ , are 5 mm and 3 mm, respectively. According to the figure, the presented procedure is considered applicable, but the following should be noted. Since it does not take account of the plastic deformation of the sheets,  $H$  will be underestimated when the ratio of the volume of the stretched part to that of the clay specimen is large. A method applicable to such a case remains to be solved.

#### 5. Some Sheet Forming Trials

Various sheet formings were attempted for relatively small articles by using the proposed process. Some examples are shown in Figs. 14 (a) ~ (e).

The result of hemispherical stretch-forming for A 1050-H24 sheets is shown at the left in Fig. 14 (a), which was obtained at the stage before fracture initiation. The die used had an aperture radius of 5 mm and a profile radius of 3 mm. The result of applying the conventional method using this die and a hemispherical-headed punch is also shown in the right

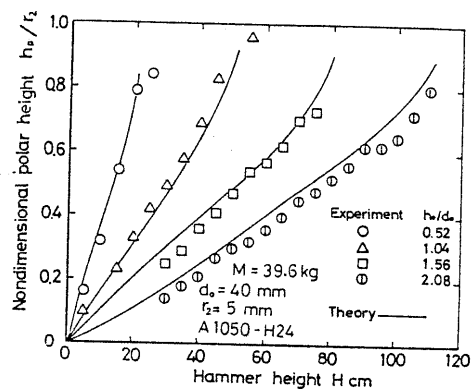
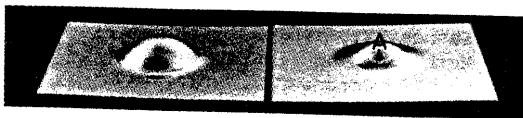


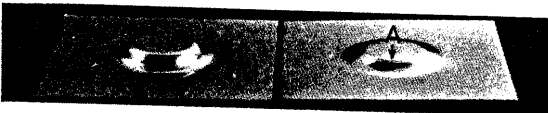
Fig. 13 Relation between the nondimensional polar height  $h_p/r_2$  and the fall height of the hammer  $H$ .

of the figure, which was obtained after necking initiation. Employing the same die as this but with the bottom closed, an attempt of flat-bottomed stretch-forming was made. The result is given at the left in Fig. 14 (b), while the result of applying the conventional method using a flat-headed punch with a radius of 4.7 mm and a profile radius of 1 mm is presented at the right in the figure. It is seen that the limit forming heights in the authors' process are higher than those by the conventional approach; they have been enhanced by more than 20 percent in Fig. 14 (a) and 50 percent in Fig. 14 (b), respectively. The reason for such an advantage is that the pressure distributes more uniformly in the authors' process than in the conventional method, and thus the strain is less localized in the former.

Using an aluminum foil AlN-H28 0.1 mm in thickness, conical-cup forming was attempted with a cone angle  $\theta = 90^\circ$ . A similar comparison to that in Figs. 14(a) and (b) is made in Fig. 14 (c). In the case of the conventional method, either wrinkling or fracture occurs before the



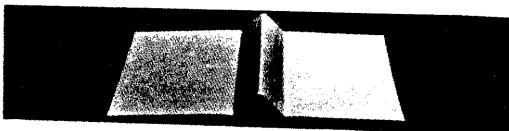
Clay ( $r_2 = 5$ ) Hemispherical-headed punch  
( $d_1 = 9.4$ ,  $r_p = 4.7$ )  
(a) Stretch-forming (hemispherical)



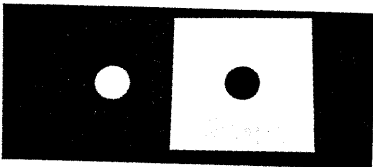
Clay ( $r_2 = 5$ ) Flat-headed punch  
( $d_1 = 9.4$ ,  $r_p = 1.0$ )  
(b) Stretch-forming (flat-bottomed)



Clay ( $d_2 = 22$ ,  
 $d_f = 14$ ,  $\theta = 90^\circ$ ) Conical-headed punch  
( $d_1 = 20$ ,  $d_f = 14$ ,  
 $\theta = 90^\circ$ )  
(c) Conical-cup forming



(d)  $90^\circ$ -V bending



(e) Blanking and piercing ( $\phi 20$ )

A: necking, B: fracture, C: wrinkling,  
Unit: mm.

Fig. 14 Various applications of the proposed process.

forming height attains 4 mm, irrespective of various blank-holding forces and blank sizes. On the other hand, successful forming is achieved by selecting an adequate forming condition in the authors' method. This example indicates that a certain drawing for metal foil is possible without use of any punch and blank-holder. Figure 14 (d) illustrates an example of  $90^\circ$ -V bending for the A 1050-H24 sheet, which suggests that an excellent fluidity of the clay material enables us to obtain a sharp corner. Blanking of a disk and piercing of a hole from A 1050-H24 sheets are illustrated in Fig. 14 (e), where their diameters are 20 mm. The result indicates that if a sufficient high pressure is obtained, the present method can serve as a shearing process for relatively small blanks and holes.

Though the characteristics of the proposed process have not been clarified sufficiently yet, a few advantages of the process can be mentioned. Since a punch and a blank-holder are not used, the equipment is simplified; the forming operation is simple; formability is improved in stretch-forming of half-hard sheets or drawing of foils. Accordingly, it can be concluded that the process is promising as a new forming technique. However, since the clay material employed in the present research happened to be adhesive to the die and metal sheets, some releasing measures had to be taken in practice. This problem remains to be solved in future investigations.

## 6. Conclusions

As the first step to develop a new type of sheet metal forming process applicable to small batch production, a dynamic compression test of clay cylinders was carried out, using a drop hammer apparatus, and the contact pressure generated was examined. Results obtained are summarized as follows:

(1) A peak value of the contact pressure was measured at each radial position and was denoted by  $p$ . It distributed in a similar way to the so-called friction-hill phenomenon along the radial direction and always became maximum near the specimen center. The  $p$  value therein increased with an increase of the fall height of the hammer and with a decrease of the specimen volume and its relative height. Under a constant potential energy of the hammer, a large mass is preferable for raising  $p$ .

(2) A considerable pressure level could be realized in the proposed method. The maximum pressure gained in the present experiment is 60 MPa (612 kgf/cm<sup>2</sup>), which amounts to a factor of about 750 of the quasi-static compressive stress. However, since the high pressure is limited to the center region of the specimen, the method is recommendable for sheet forming of small articles.

(3) An experimental equation was obtained which can express precisely the relation between the mean compressive stress  $\bar{Y}_m$  and the mean compressive strain rate  $\dot{\bar{\epsilon}}_m$  throughout a wide range of the test con-

ditions. An approximately proportional relation  $p_0 = 2.92Y_m$  was also found between  $Y_m$  and the maximum pressure  $p_0$ . On the basis of this relation, a procedure for estimating  $p_0$ , necessary for determining the forming condition, was presented. The  $p_0$  value was predicted within an error of  $\pm 10$  percent. The aforementioned proportional relation was theoretically proved.

(4) As a result of the investigation as to the applicability, the following advantages were found: the punch and the blank-holder are not needed; forming operation is simple; its stretchability is improved for half-hard sheets as compared with that in the conventional process; a conical forming of foils which is impossible by the conventional method is possible on account of the pressure laterally acting. An improvement in releasability of the medium from the die and metal sheets is desirable.

#### Appendix

The relation between the mean compressive stress  $\bar{Y}$  and the compressive strain  $\epsilon$  in dynamic compression of cylindrical specimens is derived in the following. Neglecting barrelling, the following constitutive equation is employed.

$$\bar{Y} = c' \dot{\epsilon}^p \epsilon^q, \quad (11)$$

where the constants  $c'$ ,  $p$  and  $q$  depend on mechanical properties of the specimen, friction on the specimen-platen interface and the redundant work. The nominal strain rate  $\dot{\epsilon}$  is defined as

$$\dot{\epsilon} = de/dt = d((h_0 - h)/h_0)/dt = v/h_0. \quad (12)$$

The equation of motion for the hammer is given by

$$-M dv/dt = A \bar{Y}, \quad (13)$$

where  $A$  is the current cross-sectional area of the specimen. Substituting Eqs. (11) and (12) into Eq. (13) gives

$$d\dot{\epsilon}/\dot{\epsilon}^{p-1} = B \epsilon^q d\epsilon, \quad (14)$$

where  $B = -A_0 c' / (M \dot{h}_0)$ , and  $A_0$  is the initial cross-sectional area of the specimen. Using the initial condition  $\dot{\epsilon} = \dot{\epsilon}_0$  at  $\epsilon = 0$  and integrating Eq. (14), we find

$$\dot{\epsilon}^{2-p} = \dot{\epsilon}_0^{2-p} + B(2-p)\epsilon^{q+1}/(q+1). \quad (15)$$

Noting  $\dot{\epsilon} = 0$  at the end of compression, the final strain  $\epsilon_1$  is expressed from Eq. (15) as

$$\epsilon_1 = \{[(q+1)\dot{\epsilon}_0^{2-p}/(B(p-2))]\}^{1/(q+1)}, \quad (16)$$

Substituting the expression for  $\dot{\epsilon}$  from (15) into Eq. (11), we obtain

$$\bar{Y} = c' [\dot{\epsilon}_0^{2-p} + B(2-p)\epsilon^{q+1}/(q+1)]^{p/(2-p)} \epsilon^q. \quad (17)$$

When the compression condition is specified,  $Y_m$  can be calculated from Eqs. (5)', (6) and (16), and  $\dot{\epsilon}_m$  also from Eqs. (4) and (16). The constants in Eq. (11) were determined by fitting the computed  $Y_m - \dot{\epsilon}_m$  relation to the experimental, and thus the equation

$$\bar{Y} = 0.025 \dot{\epsilon}^{1.25} \epsilon^{1.1} \text{ (MPa)} \text{ was obtained.}$$

#### References

- (1) Fukuda, M. and Yamaguchi, K., Journal of JSTP (in Japanese), Vol. 21, No. 235 (1980-8), p. 727.
- (2) Nakamura, K. and Nakagawa, T., Press Technique (in Japanese), Vol. 19, No. 9 (1981-8), p. 60.
- (3) Kasuga, Y., Theory of Plasticity and Metal Forming (in Japanese), (1968), p. 139, Corona Co., Ltd.
- (4) Samanta, S.K., Int. J. Mech. Sci., Vol. 9 (1967), p. 485.
- (5) Aku, S.Y., Slater, R.A.C. and Johnson, W., *ibid.*, Vol. 9 (1967), p. 495.
- (6) Slater, R.A.C., Johnson, W. and Aku, S.Y., *ibid.*, Vol. 10 (1968), p. 169.
- (7) Hawkyard, J.B. and Potter, T.B., *ibid.*, Vol. 13 (1971), p. 171.
- (8) Kasuga, Y., Theory of Plasticity and Metal Forming (in Japanese), (1968), p. 189, Corona Co., Ltd.
- (9) Takahashi, K., Trans. Japan Soc. Mech. Engrs. (in Japanese), Vol. 36, No. 289 (1970-9), p. 1444.